ELSEVIER

Journal of Photochemistry and Photobiology A: Chemistry 144 (2001) 237–243

Journal of Photochemistry and Photobiology A:Chemistry

www.elsevier.com/locate/jphotochem

Photochemical processes: potential energy surface topology and rationalization using VB arguments

Michael A. Robb [a,*], Massimo Olivucci [b,1]

[a] *Department of Chemistry, King's College London, Strand, London WC2R 2LS, UK*
[b] *Dipartimento di Chimica, Università degli Studi di Siena, Via Aldo Moro, I-53100 Siena, Italy*

Received 22 December 2000; received in revised form 28 February 2001; accepted 2 March 2001

Abstract

The development of quantum chemical methods capable of treating excited and ground states of organic molecules in a balanced way has prompted many applications in the field of mechanistic organic photochemistry. In this paper, we review a few representative computational results which illustrate the currently emerging concept of a photochemical (and photophysical) reaction pathway. In particular, we focus on the shape (topology) of the potential energy surface along the excited state branch of the reaction path as well as on the shape and nature of the photochemical funnel where decay to the ground state occurs. The chemical effect of different topologies and their origin in terms of simple valence bond ideas are discussed.

Keywords: Photochemistry; Reaction mechanism; Conical intersection; Computational chemistry

1. Introduction

In photochemical processes (for some recent theoretical reviews see [1–4]), the reactant resides on an excited state potential energy surface and the product accumulates on the ground state. Thus, the reaction path must have at least two branches: one located on the excited state potential energy surface and the other located on the ground state potential energy surface. In general, these branches are connected via a "funnel" [5–8] where the excited state reactant or intermediate is delivered to the ground state. The goal of theoretical and computational approaches, in the study of photochemical mechanisms, is the description of what happens at the molecular level from energy absorption to product formation [8]. This involves the description of the reaction co-ordinate from the Franck–Condon (FC) point, located on the potential energy surface of the spectroscopic state, to the photoproduct energy valley located on the ground state potential energy surface.

In this paper, we review some of our recent work where the reaction path has been mapped out for photochemical pathways of interest in both chemical physics (where detailed results from time-resolved spectroscopy are available) and in organic chemistry (where, usually, detailed product analysis data are available). We will focus on the conceptual basis of the subject (the way in which the topology of the potential energy surface can control reactivity). We will also show that the computed potential energy surface structure can be rationalized (or sometimes predicted) in terms of simple valence bond arguments. We begin with a brief summary of the theoretical methods that can be used for computational studies of excited state problems.

2. Modeling photochemical and photophysical processes

The tools for modeling excited state processes have been developed over the last 10 years and are now available in standard quantum chemistry packages. Space limitations in this paper preclude a detailed discussion and we refer the reader to our recent review [3,4] for a more complete survey. Accordingly, we will limit our discussion to a brief mention of those methods that we have developed and which are distributed as part of standard software, such as the Gaussian package [9]. Since one needs a balanced representation of ground and excited states, standard methods, such as RHF, MP2 and DFT are, in general, not applicable. Methods,

* Corresponding author. Tel.: +44-20-7848-2098; fax: +44-20-7848-2810/2284.
E-mail addresses: mike.robb@kcl.ac.uk (M.A. Robb), olivucci@unisi.it (M. Olivucci).
[1] Tel.: +39-577-234274/80; fax: +39-577-234278.

1010-6030/01/$ – see front matter
PII: S1010-6030(01)00453-1

such as CASSCF [10] and multi-reference perturbation methods [11,12] (CAS-MP2, CASPT2 and MS-CASPT2) are essential. Using these methods, the excited and ground state reaction paths can be mapped out and the reaction energetics can be predicted with a level of accuracy that allows comparison with the experiment. The new tools required for investigation of photochemical reaction paths (mainly based on the use of CASSCF gradients) relate to:

1. Characterizing the potential energy region of the "photochemical funnel" — the key mechanistic element of photochemical reactions [13]. This is accomplished by locating and optimizing the structure of the conical intersections (CI) and singlet/triplet crossings (STC) associated to this entity.
2. Locating reaction paths departing from the FC point or from the CI point [14].
3. On-the-fly dynamics studies that follow the evolution of the system according to Newtonian dynamics using the gradient of the electronic wavefunction (see, for example [15–17]).

3. How does potential surface topology control photochemical and photophysical processes?

Photochemical or photophysical transformations are non-adiabatic processes. The reaction co-ordinate begins on the excited state reached after photoexcitation and terminates on the ground state. The reaction co-ordinate must thus comprise one or more points where a radiationless (or non-adiabatic) event occurs and the system decays from an upper potential energy surface to a lower potential energy surface. In certain cases, this point occurs after the bond-breaking/bond-making processes characterizing the reaction have been completed. In this case the photochemical reaction is "adiabatic" in the sense that it occurs entirely on a "single" excited state potential energy surface. However, in other cases the bond-breaking/bond-making process occurs in correspondence of the decay and is characterized by the topology, molecular and electronic structure of the funnel. When the excited and ground state have the same spin multiplicity this funnel corresponds to a CI. On the other hand, when the excited and ground state have different spin multiplicity (e.g. triplet and singlet), the funnel corresponds to a crossing (e.g. a singlet triplet crossing STC). Some of the possibilities are illustrated in Fig. 1.

In general, the evolution of the excited state reactant depends on the topology of the funnel and the topology of the excited state potential energy surface. For instance, a conical intersection can be "peaked" as shown in Fig. 1a, b, d and f or "sloped" as shown in Fig. 1c and e. If there is no barrier in the reaction co-ordinate on S_1 (Fig. 1b, d, e and f) then the reaction may be ultrafast. Such processes are candidates for study using femtochemical methods. They can also be modeled with on-the-fly dynamics. If there is a barrier on the reaction co-ordinate (Fig. 1a and c) then the excited state process is activated and one may observe temperature or wavelength dependent photochemistry. The sloped conical intersection topology (Fig. 1c) is interesting. Reaching the surface crossing is not really an activated process of the type normally encountered in thermochemistry. Even if there is sufficient energy to access the surface crossing, the system may oscillate between excited and ground states in the crossing region for some considerable time before decay to the ground state occur. The rate of the reaction may thus be slower than that predicted on the basis of the energy barrier. This is in contrast to the peaked intersection

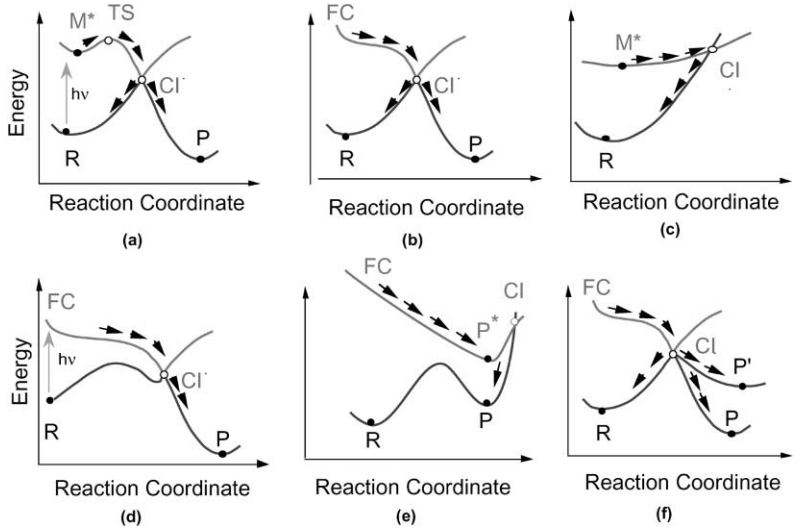

Fig. 1. Schematic representation of the reaction path topology and position of the photochemical funnel (a conical intersection) along the reaction co-ordinate: (a) Transition state (TS) before a peaked conical intersection; (b) barrierless path with a peaked conical intersection; (c) path with a sloped conical intersection; (d) as for a or b but with an intersection on the product side of the reaction co-ordinate, (e) as for c but with an intersection on the product side of the reaction co-ordinate; (f) as for a or b but with multiple competitive ground state relaxation paths.

where, once the crossing is reached, decay to the ground state takes place on a time scale of less than a vibration.

The process of photoproduct formation is affected by the position of the funnel along the reaction co-ordinate and the number and orientation of the ground state relaxation paths departing near the funnel (these paths define ground state valleys that originate at the CI and end at a different photoproduct energy minima). One can see that if the conical intersection occurs on the product side of the reaction co-ordinate (Fig. 1d and e), one has an excited state adiabatic reaction which can be substantially completed before the non-adiabatic event occurs returning the system to the product region. In this case, the reaction rate may be controlled by an excited state energy barrier (not shown in Fig. 1d–e). Provided, there is a substantial thermal barrier to the thermal back reaction then one can have an enhanced product yield. Topologies of the form Fig. 1d and e can be important for photochromism. In different cases, multiple ground state relaxation paths have been located departing from the same peaked CI which leads to different photoproducts (see Fig. 1f for the case of two competitive product formation paths leading to P and P′). In these cases two or even more photoproducts could be formed starting from a single excited state reaction co-ordinate. The presence of a transition state on the S_1 surface provides a "bottleneck" which can result in an enhanced flux in the direction of one particular photoproduct. In fact, provided that the conical intersection and the product lie in the same "direction", then the production of product will be enhanced. We shall return to illustrate these ideas with some examples subsequently. But first it is useful to discuss the origin of funnels.

4. Rationalization of potential surface topology using VB arguments

Many of the funnels that we have been able to document can be understood on the basis of simple VB arguments. Here we also try to make a qualitative connection with the companion article of Haas and co-workers in this same workshop issue.

We shall try to illustrate the main ideas by classifying, loosely, conical intersections into four types (there are surely more, but many of the examples we have studied fall into these classes).

1. Three electron H_3-like triangle.
2. *Trans*-annular π bonds.
3. Charge-transfer (e.g. TICT).
4. The n–π^* re-coupling.

This classification provides the guideline to predict the structure of different conical intersections. We begin with a brief discussion of type 1–4 and then in a subsequent section we shall discuss the position and the origin of conical intersections with some examples.

In Fig. 2, we show the characteristic three electron H_3-like (type 1) conical intersection that is typical of polyenes [18], benzenes [19] and other hydrocarbons (see, for example [20]). This type of conical intersection also provides an opportunity to discuss some general ideas about conical intersections. In the H_3-like (type 1) conical intersection there are three electrons in an approximately triangular arrangement with a fourth electron acting as a spectator and residing in a fragment π-orbital (e.g. an allyl, pentadienyl, etc. fragment). In polyenes, the triangular fragment at the center of

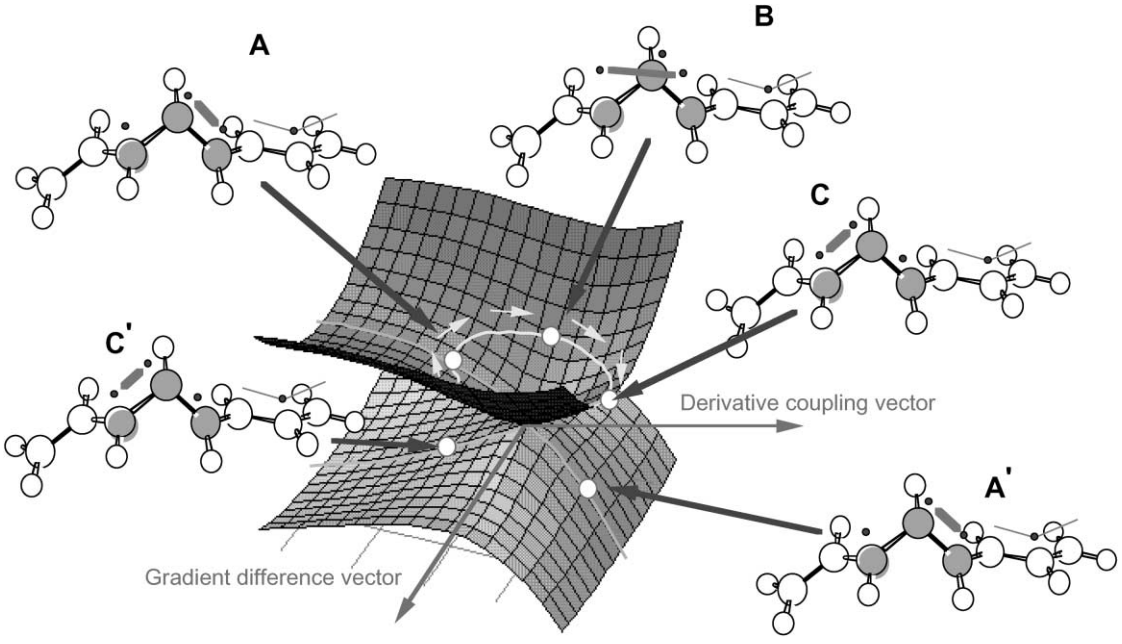

Fig. 2. The VB structures for an H_3-like conical intersection in a hydrocarbon chain (the position of the corresponding "kink" is indicated by shaded atoms).

the conical intersection structure corresponds to a kink located along the chain (see Fig. 2). In general, there are two molecular modes (parallel to the derivative coupling and gradient difference vectors between the upper and lower states) that lift the upper state/lower state degeneracy. In type 1, conical intersection the degeneracy remains for geometric distortions orthogonal to these directions, so that the "point" in Fig. 2 becomes a hyperline (a f-2 dimensional space where f is the number of vibrational degrees of freedom of the molecule) in f dimensions. The gradient difference is "quasi-totally symmetric" while the derivative coupling is "quasi-non-totally symmetric". Thus, moving along the gradient, difference directions preserves the approximate C_{2v} structure of the triangle while movement along the derivative coupling direction retains only approximate C_s symmetry. There are two linearly independent VB couplings of three electrons in three orbitals. These are indicated as A and B in Fig. 2. VB structure C is a linear combination of A and B. As one moves on a circle (see arrows in Fig. 2), remaining on the upper surface, the VB coupling changes A → B → C through the linear combinations of the two linearly independent VB couplings of three electrons in three orbitals. Moving from the left of the upper surface (A) through to the right of the lower surface (A′), one preserves the VB coupling. This VB coupling provides the force field that drives the geometrical change. These ideas have been used recently by Haas in an attempt to predict the photochemical behavior from ground state surface topology. For H_3 itself, the information needed for what Haas calls "anchor points" would be the three possible degenerate $H_2 + H$ pairs. These pairs can be related to the three different spin coupling schemes discussed above. The three pairs would correspond to the anchor points of a Haas diagram, and the equilateral triangle conical intersection will be confined within these three nodes. However, in polyenes, the unusual kink structure may be completely distorted and not easily related to ground state equilibrium structures and intermediates. This is expected to diminish the predictive ability of Haas method.

When more than four electrons are involved in the coupling/re-coupling process at a conical intersection, the arguments are less easily stated. However, conical intersections in bicyclic π electron systems can still be qualitatively understood. Azulene [21] provides an example of type 2 system and involves a sloped conical intersection and the reaction path topology of Fig. 1b. The ground state is a delocalized system with a *trans*-annular single bond (see Fig. 3a). In the excited state, one has a biradical structure (Fig. 3b) with a *trans*-annular double bond. Compressing the *trans*-annular single bond from the ground state (S_0) equilibrium value drives the S_0 energy up steeply while it lowers the energy for double bond on the excited state (S_1). Thus, one reaches the intersection structure shown in Fig. 3c along a bond compression co-ordinate. In this system the gradient difference mode corresponds to the quasi-totally symmetric motion of the *trans*-annular bond (Fig. 3d) while the non-totally symmetric derivative coupling mode (Fig. 3e) is the motion that moves towards the localized VB structures of the ring.

Type 3 conical intersections (i.e. the charge transfer type) are ubiquitous. The polymethine cyanine dyes in Fig. 4a is a simple example [22], while biological chromophores, such as the different homologues of the retinal protonated Schiff (PSBs) base is another example that has been documented in detail [23]. For cyanines and PSBs, the conical

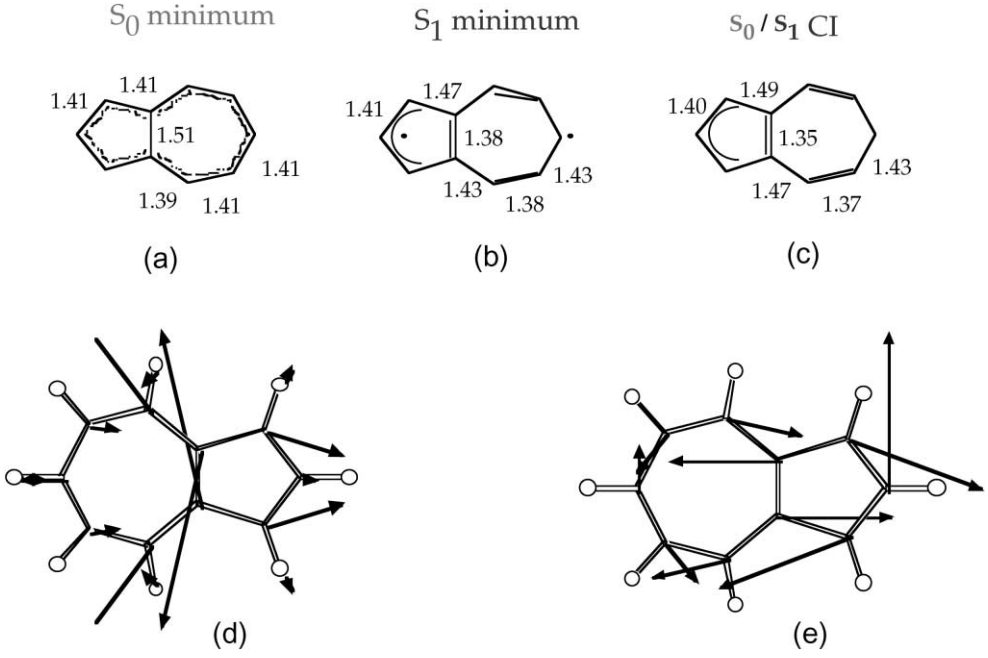

Fig. 3. Azulene conical intersection: (a–c) molecular geometries and VB structures; (d) gradient difference vector; (e) derivative coupling vector.

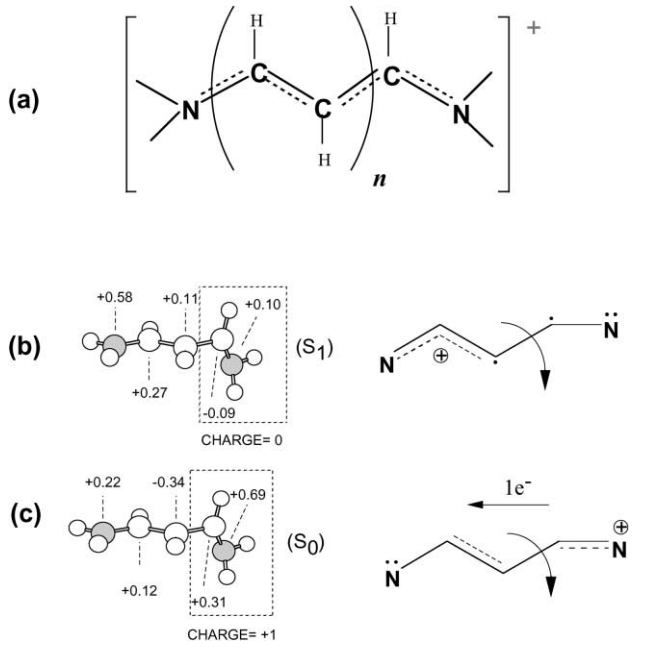

Fig. 4. Conical intersection in cyanines: (a) general structure of polymethine cyanines; (b and c) molecular geometries, VB structures and charges of the trimethine cyanine conical intersection. The total charge of the framed moiety of the molecule is also given.

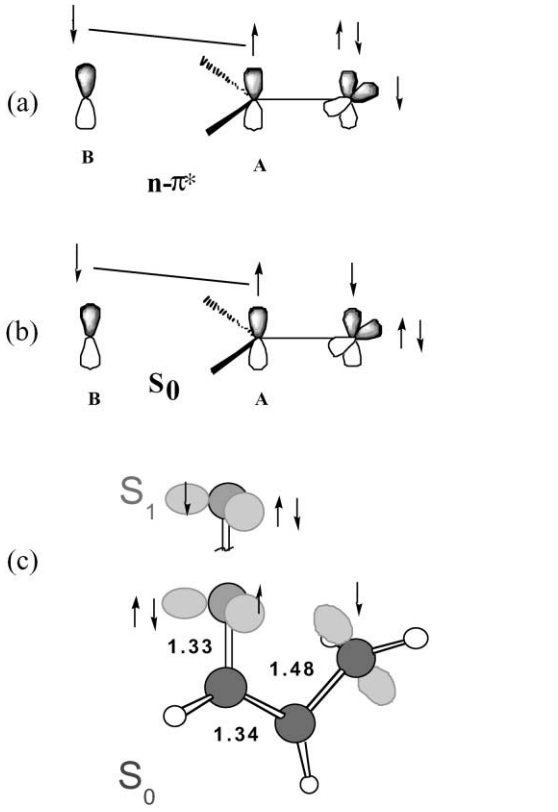

Fig. 5. $S_0/S_1(n–\pi^*)$ conical intersections: (a and b) schematic VB structures; (c) the example of acrolein.

intersection occurs roughly halfway along a *cis–trans*-isomerization co-ordinate at the geometry given in Fig. 4b and c for thrimethine cyanine. At this geometry, the ground state S_0 and excited state S_1 cross. The resonance structures for the degenerate S_0 and S_1 states of this model cyanine are shown in the same figures. At the conical intersection geometry these structures correspond to that of a "classic" twisted internal charge transfer (TICT) structure where the two halves of the twisted molecule differ by the charge of one electron. The occurrence of an S_0/S_1 intersection (i.e. an energy degeneracy) can be rationalized on the basis of the fact that these systems correspond to heterosymmetric diradicaloids [24] where the energies of certain frontier orbitals of two weakly interacting moieties are equal. For instance, in our cyanine model containing six π-electrons, the SOMO energy of the $H_2N–CH–CH–$ moiety taken with three π-electrons and the LUMO energy of the $–CH–NH_2$ moiety taken with two π-electrons, is equal at the optimized CI structure (see Fig. 4c). As a consequence, the placement of the sixth π-electron on either the moiety (yielding the resonance structures of Fig. 4c and b, respectively) will result in the same stabilization.

Finally, the type 4 conical intersection for $S_0/S_1(n–\pi^*)$ systems is also easily rationalized. Consider the model system shown in Fig. 5a and b and comprising a carbonyl group interacting with a singly occupied p_z orbital. When the singly occupied carbonyl carbon p_z orbital (A in Fig. 5a and b) becomes coupled to that of the adjacent carbon center (B in Fig. 5a,b), and decoupled from the oxygen (O) center, then the $(O_{p_z})^1(O_{p_x})^2$ and $(O_{p_z})^2(O_{p_x})^1$ configurations of the oxygen atom become degenerate in energy. This type of coupling operates in acrolein [25]: the simplest α,β-enone. In Fig. 5c, we report the geometry of the $S_0/S_1(n–\pi^*)$ conical intersection of acrolein together with the VB couplings for S_0 and S_1 states. The twisted position of the terminal methylene group, allows the formation of a double bond between the remaining (central) two carbons, leaving the O atom isolated. This type of conical intersection can be easily related to the ground state relaxation path and VB recoupling scheme leading to oxetane formation (a four membered heterocyclic compound with one oxygen atom) or even *cis–trans*-isomerization when the α,β-double bond is substituted. In particular, the cyclization involves interaction of the oxygen atom in its S_1 configuration (see Fig. 5c) with the unpaired electron in the terminal CH_2 group and successive C–O bond formation.

5. Conclusion

In the preceding two sections, we have revised different systems where the excited state path topology and funnel topology are different. Further, in all cases, the origin of the funnel can be understood using qualitative chemical arguments related to resonance theory (VB spin coupling arguments). This can be seen as a refinement of the correlation diagrams that are commonly used in organic photochemistry.

Table 1
Funnel (conical intersection) topologies and their VB models

Reaction or molecule	Reference	Reaction path and funnel topology (Fig. 1)						VB description of the funnel (see text)			
		1a	1b	1c	1d	1e	1f	i	ii	iii	iv
Cyanine	[22]					X				X	
PSB	[23]		X							X	
H• transfer	[24]	X								X	
Azulene	[21]			X					X		
Pentalene	[27]			X					X		
Benzene	[19]	X						X			
Cyclohexadiene/hexatriene	[28]						X	X			
β,γ-Enones	[30]				X						X

Our purpose in this section is to summarize these conceptual threads with some examples that are collected in Table 1.

A quick inspection of Table 1 shows that for a set of selected examples, most combinations of potential surface topology, conical intersection topology and VB type are found in practice. Thus, taking the charge transfer CI (type 3) as an example, for the photoisomerization of the protonated Schiff retinal [22], the CI is peaked, and occurs almost half way along the isomerization co-ordinate. In contrast, for the cyanine systems we have shown [22] that the conical intersection is sloped and occurs on the product side of the barrier. For a hydrogen transfer reaction, in reference [26], we have shown that the conical intersection lies almost halfway along the reaction co-ordinate so that the "adiabatic" photochemical transformation becomes "aborted" and the reactant may be regenerated. The variability observed in the photochemical transformation of unsaturated hydrocarbons is large. In these species the VB structure of the conical intersection is either type 1 or 2. In azulene [21], one has a sloped conical intersection of type 3 so that only a photophysical process (corresponding to radiationless deactivation) is observed. While for the cyclohexadiene/hexatriene system, the intersection is also sloped but occurs at a geometry where both product formation, reactant back-formation and, in certain substituted derivatives, bicyclic photoproduct formation is observed (this corresponds to the case of Fig. 1f). Benzene [19], has a conical intersection of type 1, in spite of being an aromatic system. The occurrence of a minimum and a transition state (Fig. 1a) is consistent with the observed wavelength dependent photochemistry. Finally, in $S_0/n–\pi^*$ systems (type iv), one also has a considerable variety. In such systems (see [29]), one also has triplet–triplet (T_1/T_2) conical intersections that occur at the same geometries as the singlet–singlet (S_0/S_1) ones and the potential surface can be very complex (see also the case of the photolysis of azoalkanes in [30]).

Acknowledgements

A NATO Grant (CRG 950748) finances the collaboration between M.A.R. and M.O.

References

[1] F. Bernardi, M.A. Robb, M. Olivucci, Chem. Soc. Rev. 25 (1996) 321–328.
[2] F. Bernardi, M. Olivucci, J. Michl, M.A. Robb, The Spectrum 9 (1997) 1–5.
[3] M.A. Robb, M. Garavelli, M. Olivucci, F. Bernardi in: K.B. Lipkowitz, D.B. Boyd (Eds.), Reviews in Computational Chemistry, Wiley, New York, Vol. 15, 2000, pp. 87–146.
[4] M. Olivucci, M.A. Robb, F. Bernardi in: J. Waluk (Ed.), Conformational Analysis of Molecules in Excited States, Wiley, New York, 2000, pp. 297–366.
[5] E. Teller, Isr. J. Chem. 7 (1969) 227–235.
[6] H.E. Zimmerman, J. Am. Chem. Soc. 88 (1966) 1566.
[7] J. Michl, Mol. Photochem. 4 (1972) 243.
[8] W. Fuss, K.L. Kompa, S. Lochbrunner, A.M. Muller, Chem. Phys. 232 (1998) 174.
[9] M.J. Frisch, G.W. Trucks, H.B. Schlegel, P.M.W. Gill, B.G. Johnson, M.A. Robb, J.R. Cheeseman, T. Keith, G.A. Petersson, J.A. Montgomery, K. Raghavachari, M.A. Al-Laham, V.G. Zakrzewski, J.V. Ortiz, J.B. Foresman, J. Cioslowski, B.B. Stefanov, A. Nanayakkara, M. Challacombe, C.Y. Peng, P.Y. Ayala, W. Chen, M.W. Wong, J.L. Andres, E.S. Replogle, R. Gomperts, R.L. Martin, D.J. Fox, J.S. Binkley, D.J. Defrees, J. Baker, J.P. Stewart, M. Head-Gordon, C. Gonzalez, J.A. Pople, Gaussian 94, Gaussian, Inc., Pittsburgh, PA, 1995.
[10] B.O. Roos, in: K.P. Lawley (Ed.), Advanced Chemistry and Physics (Ab Initio Methods in Quantum Chemistry, Part II), Wiley, New York, 1987, Vol. 69, pp. 399–446.
[11] J.J. McDouall, K. Peasley, M.A. Robb, Chem. Phys. Lett. 148 (1988) 183.
[12] K. Andersson, P.A. Malmqvist, B.O. Roos, J. Chem. Phys. 96 (1992) 1218.
[13] M.J. Bearpark, M.A. Robb, H.B. Schlegel, Chem. Phys. Lett. 223 (1994) 269.
[14] P. Celani, M.A. Robb, M. Garavelli, F. Bernardi, M. Olivucci, Chem. Phys. Lett. 243 (1995) 1–8.
[15] M.J. Bearpark, F. Bernardi, S. Clifford, M. Olivucci, M.A. Robb, B.R. Smith, J. Am. Chem. Soc. 118 (1996) 169–175.
[16] T. Vreven, F. Bernardi, M. Garavelli, M. Olivucci, M.A. Robb, H.B. Schlegel, J. Am. Chem. Soc. 119 (1997) 12687–12688.
[17] S. Klein, M.J. Bearpark, B.R. Smith, M.A. Robb, M. Olivucci, F. Bernardi, Chem. Phys. Lett. 293 (1998) 259–266.
[18] M. Olivucci, I.N. Ragazos, F. Bernardi, M.A. Robb, J. Am. Chem. Soc. 115 (1993) 3710–3721.
[19] I.J. Palmer, I.N. Ragazos, F. Bernardi, M. Olivucci, M.A. Robb, J. Am. Chem. Soc. 115 (1993) 673–682.
[20] P. Celani, S. Ottani, M. Olivucci, F. Bernardi, M.A. Robb, J. Am. Chem. Soc. 116 (1994) 10141–10151.

[21] M.J. Bearpark, F. Bernardi, S. Clifford, M. Olivucci, M.A. Robb, B.R. Smith, J. Am. Chem. Soc. 118 (1996) 169–175.
[22] A. Sanchez-Galvez, P. Hunt, M.A. Robb, M. Olivucci, T. Vreven, H.B. Schlegel, J. Am. Chem. Soc. 122 (2000) 2911–2924.
[23] M. Garavelli, F. Bernardi, M. Olivucci, T. Vreven, S. Klein, P. Celani, M.A. Robb, Faraday Discuss. 110 (1998) 51–70.
[24] J. Michl, V. Bonacic-Koutecky, Electronic Aspects of Organic Photochemistry, Wiley, New York, 1990.
[25] M. Reguero, M. Olivucci, F. Bernardi, M.A. Robb, J. Am. Chem. Soc. 116 (1994) 2103–2114.
[26] W.M. Nau, G. Greiner, J. Wall, H. Rau, M. Olivucci, M.A. Robb, Angew. Chem. Int. Ed. 37 (1998) 98–101.
[27] M.J. Bearpark, F. Bernardi, M. Olivucci, M.A. Robb, Int. J. Quantum Chem. 69 (1996) 505–512.
[28] P. Celani, F. Bernardi, M.A. Robb, M. Olivucci, J. Phys. Chem. 100 (1996) 19364–19366.
[29] S. Wilsey, M.J. Bearpark, F. Bernardi, M. Olivucci, M.A. Robb, J. Am. Chem. Soc. 118 (1996) 176–184.
[30] N. Yamamoto, M. Olivucci, P. Celani, F. Bernardi, M.A. Robb, J. Am. Chem. Soc. 120 (1998) 2391–2407.